

# ALOE: Action-Level Off-Policy Evaluation for Vision-Language-Action Model Post-Training

Rushuai Yang<sup>1,2\*</sup> Hecheng Wang<sup>1,3\*</sup> Chiming Liu<sup>1†</sup>

Xiaohan Yan<sup>1</sup> Yunlong Wang<sup>1</sup> Xuan Du<sup>1</sup> Shuoyu Yue<sup>1</sup> Yongcheng Liu<sup>1</sup> Chuheng Zhang<sup>4</sup>

Lizhe Qi<sup>3</sup> Yi Chen<sup>2</sup> Wei Shan<sup>1</sup> Maoqing Yao<sup>1</sup>

<sup>1</sup>AgiBot <sup>2</sup>The Hong Kong University of Science and Technology <sup>3</sup>Fudan University <sup>4</sup>Independent Researcher

\*Equal Contribution †Corresponding Author

**Abstract**—We study how to improve large foundation vision-language-action (VLA) systems through online reinforcement learning (RL) in real-world settings. Central to this process is the value function, which provides learning signals to guide VLA learning from experience. In practice, the value function is estimated from trajectory fragments collected from different data sources, including historical policies and intermittent human interventions. Estimating the value function of current behavior quality from the mixture data is inherently an off-policy evaluation problem. However, prior work often adopts conservative on-policy estimation for stability, which avoids direct evaluation of the current high-capacity policy and limits learning effectiveness. In this paper, we propose ALOE, an action-level off-policy evaluation framework for VLA post-training. ALOE applies chunking-based temporal-difference bootstrapping to evaluate individual action sequences instead of predicting final task outcomes. This design improves effective credit assignment to critical action chunks under sparse rewards and supports stable policy improvement. We evaluate our method on three real-world manipulation tasks, including smartphone packing as a high-precision task, laundry folding as a long-horizon deformable-object task, and bimanual pick-and-place involving multi-object perception. Across all tasks, ALOE improves learning efficiency without compromising execution speed, showing that off-policy RL can be reintroduced in a reliable manner for real-world VLA post-training. Videos and additional materials are available at our project website <https://rooshy-yang.github.io/aloe>.

## I. INTRODUCTION

Vision-language-action (VLA) models have emerged as a promising paradigm for robotic manipulation, enabling policies to condition actions on both real-world visual observations and natural language instructions [1, 5, 4, 52, 57, 26, 44, 25]. Recent progress has shown that combining imitation learning with reinforcement learning (RL) can substantially improve task performance beyond supervised learning [14, 51, 15, 12]. A key factor behind these improvements is the value function, which evaluates action quality and provides optimization signals for VLA policies. Value functions play a central role in RL by reducing variance and improving sample efficiency [43, 42]. However, accurately estimating value functions in real-world VLA systems remains particularly challenging [14, 32]. Unlike training on simulation, real-world RL for VLA systems faces practical constraints such as data scarcity, partial observation on real-world dynamics, and limited environment

parallelism. These factors make large-scale data collection costly and slow down RL iteration for policy convergence. Moreover, real-world VLA datasets typically consist of a heterogeneous mixture of sources, including rollouts from online deployment, corrective interventions from human operators in response to errors or unsafe behaviors, and historical data from earlier policies or pre-collected demonstrations. In such settings, value estimation for current VLA policy is inherently an off-policy problem, but it can suffer from error accumulation due to distributional uncertainty [19, 47], leading to biased estimates and unstable learning dynamics. To maintain stability for high-capacity VLA systems, prior work often adopts conservative learning strategies based on on-policy value estimation [14, 36]. Some compromise approaches such as AWR and RECAP [36, 14] relax strict on-policy requirements. In these methods, the learned value function is not intended to directly evaluate the current policy being optimized. Instead, it estimates the expected return of an implicit policy induced by training data from multiple sources. As a result, the value function may not correspond to any single executable policy, but rather reflects the average behavior distribution on which it is trained and is used to guide current policy behavior.

While this on-policy estimation design improves training stability, its application to real-world VLA systems relies on a strong assumption: the behavior distribution of the evolving policy remains close to the mixture distribution represented in the replay buffer. This assumption is particularly fragile in real-world VLA settings where human interventions, policy updates, and environment variability continuously shift the data distribution. Under this assumption, the value function trained on historical data can serve as an approximate proxy for evaluating the current policy’s actions. However, when the VLA policy evolves and its behavior distribution deviates substantially from that mixture, the learned value function may no longer reflect the true value of the current policy. This leads to misleading optimization signals and potentially incorrect training directions. For example, when a policy learns new recovery behaviors that were absent in historical data, the value function trained on past trajectories may underestimate these actions. This discourages exploration of corrective be-

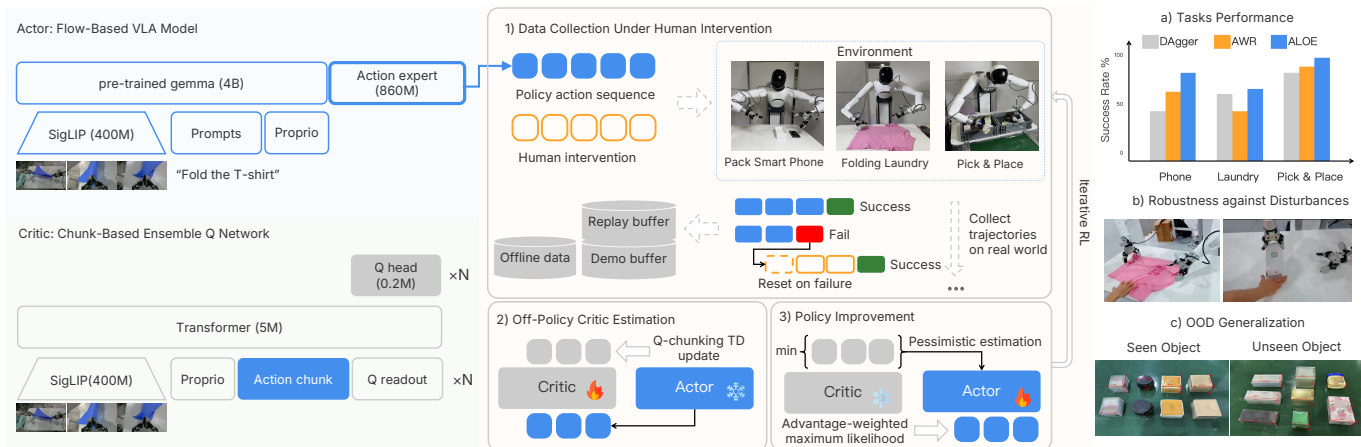


**Fig. 1: Overview of our real-world actor-critic framework for VLA post-training.** *Left*: Our method adopts an actor-critic framework in which the actor is a flow-matching-based foundation VLA model and the critic is a lightweight ensemble Q-network. The actor outputs action sequences for online real-world rollouts, while the critic predicts ensemble Q-values to assess the quality of the actor’s action chunks under the current observation. *Middle*: Real-world RL is conducted in three stages. (1) Data collection under human intervention: the VLA policy is first warm-started with offline behavior cloning and then deployed on real robots. Both successful and failed rollouts are stored in buffer. When failures or unsafe behaviors occur, a human intervenes via teleoperation to take over from the failure state and guide the robot to the goal state. (2) Off-policy critic estimation: the critic is trained on the aggregated dataset using Q-chunking TD updates. (3) Policy improvement: the actor is optimized using pessimistic value estimation and advantage-weighted maximum likelihood. *Right*: We evaluate the method on real-world manipulation tasks and demonstrate improvements in task success rate, robustness to disturbances, and zero-shot generalization to unseen objects.

haviors that are essential for robust real-world manipulation. This compromise induces a fundamental trade-off between robustness and learning efficiency in real-world VLA training, and motivating the following question:

*When can off-policy reinforcement learning be reliably applied to improve real-world VLA policies?*

In this work, we introduce ALOE, an action-level off-policy evaluation framework that enables effective off-policy policy improvement under real-world RL setting. We show that such conservatism from prior approaches is not inherent to real-world VLA training, but instead arises from specific assumptions about how value estimates are obtained and used. By explicitly addressing key sources of critic bias, the assumptions can be partially relaxed without compromising training stability. Specifically, we reintroduce traditional temporal-difference bootstrapping method to estimate the behavior quality of current policy, providing effective off-policy policy evaluation and stitch different fragments from different source. To accelerate credit propagation under long-horizon and sparse reward setting, we adopt Q-chunking for efficient reward signal backpropagation, ensuring efficient propagation of reward signals to critical action frames. To stabilize off-policy Q learning, we consider a pessimistic value estimation for uncertainty, mitigating the error accumulating on uncertain behavior. We then adopt this value function as preference signal to guide high-capacity policy update, providing stable policy improvement. Our approach allows VLA policies to

leverage fine-grained, action-level value information while preserving the robustness properties essential for real-world training. We summarize our contributions as follows:

- We propose an off-policy policy evaluation framework for real-world VLA training under human-in-the-loop data collection, enabling action-level evaluation to support reliable policy improvement.
- We develop stabilization mechanisms for action-value learning in real-world settings, enabling reliable long-horizon credit assignment for flow-based VLA policies.
- We evaluate our approach on three real-world robotic manipulation tasks, demonstrating improved task success, generalization, learning efficiency, and recovery from execution errors compared to prior VLA training methods.

## II. RELATED WORK

### A. Foundations of Policy Evaluation

Policy evaluation aims to estimate the expected long-term outcomes of actions or policies and is commonly categorized along two axes: on-policy vs. off-policy estimation, and Monte Carlo (MC) targets vs. Temporal Difference (TD) bootstrapping targets [43]. On-policy methods estimate the expected return of the action distribution induced by the data-collecting policy, ensuring alignment with the data distribution and stable learning [37, 48, 23]. In contrast, off-policy methods estimate the expected return of specific actions or target policies using data collected from different behavior policies, enabling broader action coverage and improved sample

efficiency [21, 16, 7, 55, 56]. MC-based methods rely on complete episodic returns and suffer from high variance, while TD-based methods leverage Bellman bootstrapping to learn from fragment trajectories [43]. Although off-policy, TD-based value estimation is well studied in classical RL, extending these mechanisms to high-capacity VLA models in real-world settings remains challenging [14, 47, 19]. Our work mitigates these challenges by enabling reliable action-value estimation for large diffusion- and flow-based VLA policies on more complex real-world tasks.

### B. Reinforcement Learning for Large VLA Policies

Recent work has explored scaling reinforcement learning to large VLA models on real robotic systems [45, 29, 27, 6, 22]. Many approaches adopt on-policy optimization, such as PPO or REINFORCE [49, 38, 48], prioritizing stability but limiting value estimation to the current behavior distribution. Another prevalent line of work employs trajectory-level preference or progress modeling, where a state-value function predicts task completion progress and serves as a reweighting signal for imitation-style updates [14, 53, 10, 31, 33]. While effective for stabilizing training, these methods do not explicitly evaluate individual actions and provide limited action-level guidance. Action-value and advantage-based methods for VLA have also been studied [13, 8, 18], but are largely restricted to offline RL settings with static data. In contrast, real-world VLA training typically follows an iterated RL paradigm with continuous online interaction and human-in-the-loop interventions [41, 35, 30, 20]. Existing methods in this regime generally avoid off-policy action-value estimation due to stability concerns. Our work bridges this gap by introducing a controlled, off-policy, action-level value estimation framework for more complex tasks like long-horizon clothing folding, high-precision phone packing tasks, enabling fine-grained action correction and trajectory stitching while preserving robustness under online, human-in-the-loop deployment.

## III. PRELIMINARIES

### A. Vision-Language-Action Model as an Episodic MDP

We model VLA as an episodic Markov Decision Process (MDP) [43] defined by the tuple  $(\mathcal{S}, \mathcal{A}, p, r, \gamma)$ . At each timestep  $t$ , the agent observes a state  $s_t \in \mathcal{S}$ , which includes visual observations and proprioceptive information, and receives a natural language instruction  $\ell$  specifying the task. The instruction  $\ell$  is treated as a conditioning variable of VLA. The agent selects an single action  $a_t \in \mathcal{A}$  according to a VLA policy  $\pi_\theta(a_t | s_t, \ell)$  parameterized by  $\theta$ . The environment transitions according to unknown dynamics  $p(s_{t+1} | s_t, a_t)$  and emits a reward  $r_t = r(s_t, a_t)$ . We consider episodic tasks that terminate upon either task success or failure, and denote termination by  $d_t \in \{0, 1\}$ . The discount factor is  $\gamma \in (0, 1)$ . The objective of reinforcement learning is to learn a policy that maximizes the expected discounted return of the current policy,

$$J(\pi_\theta) = \mathbb{E}_{\tau \sim \mathcal{D}, \pi_\theta} \left[ \sum_{t=0}^T \gamma^t r_t \right], \quad (1)$$

where trajectories  $\tau$  are sampled from a replay buffer  $\mathcal{D}$  containing off-policy transitions  $(s_t, a_t, r_t, s_{t+1}, d_t, \ell)$  collected by previous policies. While this objective can in principle be optimized using on-policy policy gradient methods [48, 40, 37], real-world VLA training is often constrained by costly environment parallelism, long-horizon task structure, and sparse rewards, which motivate the efficient reuse of history data.

### B. Actor-Critic Framework

Actor-critic methods [11, 42] address these challenges by maintaining two components: an actor  $\pi_\theta$  that represents the VLA policy, and a critic that estimates long-term outcomes to guide policy updates. We begin by defining the action-value function of a policy  $\pi$ . For a given state-action pair  $(s, a)$  and language instruction  $\ell$ , the action-value function is defined as

$$Q^\pi(s, a, \ell) = \mathbb{E}_\pi \left[ \sum_{t=0}^T \gamma^t r_t \mid s_0 = s, a_0 = a, \ell \right], \quad (2)$$

which represents the expected discounted return obtained by first taking action  $a$  at state  $s$  under instruction  $\ell$ , and then following policy  $\pi$  thereafter. The state-value function is defined as the expected action-value under the policy,

$$V^\pi(s, \ell) = \mathbb{E}_{a \sim \pi(\cdot | s, \ell)} [Q^\pi(s, a, \ell)], \quad (3)$$

and summarizes the expected return of state  $s$  under instruction  $\ell$  when actions are sampled from  $\pi$ . Given an action-value function  $Q(s, a, \ell)$  and a state-dependent baseline  $V(s, \ell)$ , the advantage function is defined as

$$A^\pi(s, a, \ell) = Q^\pi(s, a, \ell) - V(s, \ell), \quad (4)$$

which measures the relative quality of an action compared to the policy’s average behavior at a given state under instruction  $\ell$ . The advantage function is commonly used to guide policy improvement by increasing the likelihood of actions with positive advantage while suppressing suboptimal actions. In practice, the critic is often learned from a replay buffer  $\mathcal{D}$  containing transitions  $(s, a, r, s', d, \ell)$ .

## IV. METHOD

Our method targets real-world VLA reinforcement learning under human-in-the-loop data collection, where experience consists of fragmented and policy-mixed trajectories due to safety interventions. We decompose learning into policy evaluation and policy improvement. For policy evaluation in Sec. IV-A, we learn an off-policy action-value function using TD learning with Q-chunking and a pessimistic ensemble, enabling efficient long-horizon credit propagation and robust value estimation. For policy improvement in Sec. IV-B, we treat the critic as a relative preference signal and perform advantage-weighted policy updates. Finally, the detailed implementation in Sec. IV-C discusses how to adapt the RL framework into flow-based VLA architecture. The resulting algorithm enables reliable and data-efficient post-training of flow-based VLA policies in Algorithm 1.

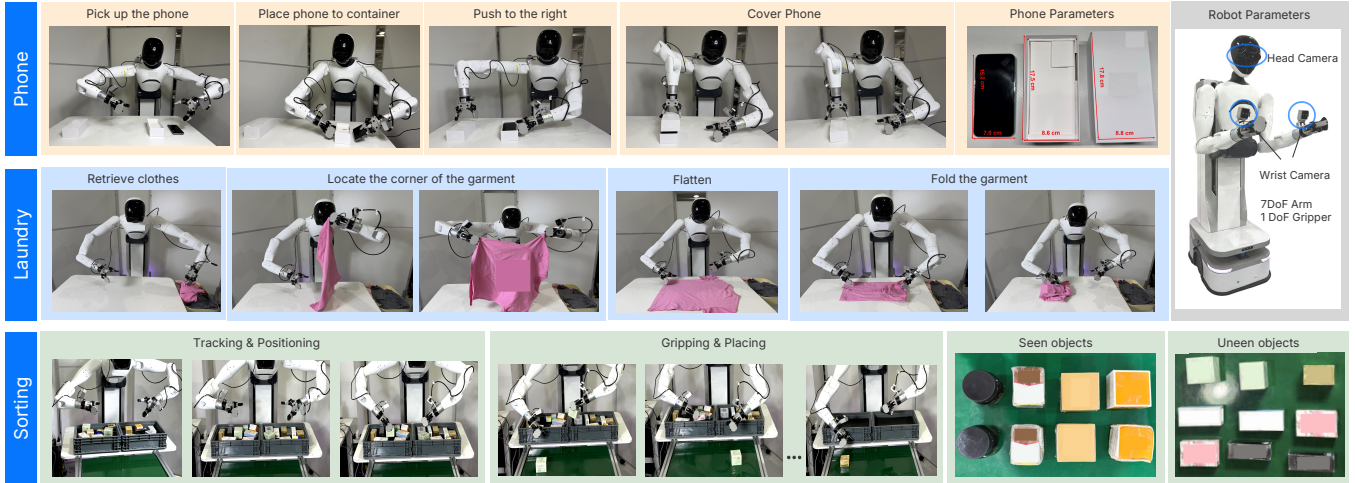


Fig. 2: Illustrations of the real-world manipulation tasks and robot setup used in our experiments. We evaluate on phone packing, laundry folding, and multi-object pick and place, showing representative task stages, object variations, and the physical robot platform with three RGB cameras.

---

**Algorithm 1** ALOE: Action-Level Off-Policy Evaluation Framework for VLA Policies

---

**Require:** initial VLA policy  $\pi_\theta$ ; critic ensemble  $\{Q_{\phi_i}\}_{i=1}^K$  with targets  $\{Q_{\phi_i^-}\}_{i=1}^K$ ; replay buffer  $\mathcal{D}$ ; discount  $\gamma$ ; hyperparameters  $(\beta, \epsilon_{\text{clip}}, \omega)$ ; update steps  $(N_Q, N_\pi)$ .

- 1: Train  $\pi_\theta$  by imitation learning on successful demonstrations.
  - 2: **for**  $k = 1$  to  $T$  **do**
  - 3:   Rollout  $\pi_\theta$  under instruction  $\ell$  with human intervention and early termination; store all transitions into  $\mathcal{D}$ .
  - 4:   **for**  $j = 1$  to  $N_Q$  **do**
  - 5:     Sample minibatch  $\mathcal{B} \subset \mathcal{D}$  and corresponding next actions from  $\pi_\theta$ .
  - 6:     Compute TD target  $y$  using Eq. (7).
  - 7:     Update critic ensemble by minimizing Eq. (8).
  - 8:     Update target networks  $\phi_i^- \leftarrow \omega \phi_i + (1 - \omega) \phi_i^-$ .
  - 9:   **end for**
  - 10:   **for**  $j = 1$  to  $N_\pi$  **do**
  - 11:     Sample minibatch  $\mathcal{B} \subset \mathcal{D}$ , and compute corresponding  $Q_{\text{pess}}(s_t, \mathbf{a}_{t:t+h}, \ell)$  using Eq. (9).
  - 12:     Estimate  $V(s, \ell)$  by sampling  $a \sim \pi_\theta(\cdot | s, \ell)$  and compute advantage using Eq. (10).
  - 13:     Compute weight  $w$  using Eq. (11).
  - 14:     Update policy  $\pi_\theta$  by minimizing Eq. (15).
  - 15:   **end for**
  - 16: **end for**
  - 17: **Return:** trained policy  $\pi_\theta$ .
- 

*A. Off-Policy Critic Estimation under Real-World Data Collection*

We first describe the policy evaluation component of our method. As shown in Fig. 1, we follow prior real-world VLA training paradigms [14, 46, 7, 36, 51]. Data is incrementally

collected through repeated rollouts of a continually evolving VLA policy. During online deployment, rollouts are frequently interrupted when the policy executes unsafe behaviors, such as collisions or joint limit violations. In such cases, the trajectory is truncated, labeled with a failure outcome, and a human operator intervenes to correct the robot’s actions before execution resumes. This process may repeat multiple times until the task is successfully completed. As a result, the replay buffer  $\mathcal{D}$  contains not only data generated by a mixture of behavior policies, but also fragmented trajectories in which different segments of a single task execution may originate from different policies or human corrections. Consequently, learning from  $\mathcal{D}$  is inherently off-policy with respect to the current actor, and long-horizon task executions are rarely observed as contiguous rollouts generated by a single policy.

Under this setting, our objective is to estimate the expected long-term outcome of taking an action at a given state under a language instruction, i.e., the action-value function in Eq. (2). A common alternative in real-world VLA systems is to use trajectory-level MC returns as a value signal [14, 23], which assign value by accumulating observed future rewards along the same trajectory and implicitly assume access to a complete trajectory suffix. In real-world training, this assumption is frequently violated due to safety-driven truncation and human intervention, resulting in fragmented task executions collected under heterogeneous behavior policies. Consequently, the future return following an action is often only partially observed, making it difficult for MC-based estimators to assign reliable credit under sparse rewards. This limitation is particularly severe in long-horizon tasks, where informative trajectory fragments must be combined across policies to reason about outcomes that are never observed as contiguous rollouts.

To mitigate these challenges, we adopt TD learning [43], which bootstraps from subsequent value estimates and allows value information to propagate backward through time. Start-

ing from the Bellman equation:

$$Q^\pi(s, a, \ell) = r + \gamma \mathbb{E}_{s' \sim p, a' \sim \pi} [Q^\pi(s', a', \ell)]. \quad (5)$$

TD learning replaces the expectation over future trajectories with a single-step target constructed from observed transitions. Given a transition  $(s_t, a_t, r_t, s_{t+1}, d_t, \ell) \sim \mathcal{D}$ , we define the TD target

$$y_t = r_t + \gamma(1 - d_t) Q_{\phi^-}(s_{t+1}, a_{t+1}, \ell), \quad (6)$$

where  $\phi^-$  denotes the parameters of a target network, and the next action is sampled from the current policy  $a_{t+1} \sim \pi_\theta(\cdot | s_{t+1}, \ell)$ .

The advantage of TD learning over MC estimation in this setting arises from the contraction property of the Bellman operator [3]. Unlike MC estimation, which requires observing a complete trajectory  $\tau = (s_t, a_t)_{t=0}^H$  to assign value to an initial state–action pair, TD learning applies the Bellman update locally at each transition. This locality allows value information to propagate incrementally through the state–action space, even when trajectories are fragmented or truncated. As a result, the process allows value information from different fragments to be implicitly stitched together, allowing the critic to aggregate credit from disjoint real-world rollouts and assign meaningful long-horizon credit without requiring contiguous task executions. This alleviates reliance on manual trajectory organization and human annotation under real-world setting. Moreover, TD learning estimates an action-conditional value function  $Q(s, a, \ell)$  instead of  $V(s)$ . This enables fine-grained, action-level credit assignment. Such action-level feedback is critical for identifying failure-prone decisions and key states in long-horizon manipulation tasks with complex intermediate dynamics.

While TD learning enables action-level credit assignment, standard one-step TD updates propagate value information backward by only a single timestep. In long-horizon manipulation tasks with sparse terminal rewards, this leads to slow credit propagation and inefficient learning, as meaningful reward signals may need to traverse about thousands of transitions. To address this issue, we adopt a Q-chunking [24] value backup that propagates value over multiple timesteps while remaining unbiased. Specifically, we define a chunked action sequence  $\mathbf{a}_{t:t+h} \triangleq (a_t, a_{t+1}, \dots, a_{t+h-1})$ , and learn a chunked action-value function  $Q(s_t, \mathbf{a}_{t:t+h}, \ell)$  that evaluates the return of executing this exact action sequence from state  $s_t$  under instruction  $\ell$ . For a transition segment  $(s_t, \mathbf{a}_{t:t+h}, r_{t:t+h-1}, s_{t+h}, \ell) \sim \mathcal{D}$ , the Q-chunking Bellman target is defined as

$$y_t^{(h)} = \sum_{k=0}^{h-1} \gamma^k r_{t+k} + \gamma^h \mathbb{E}_{\mathbf{a}' \sim \pi_\theta(\cdot | s_{t+h}, \ell)} [Q_{\phi^-}(s_{t+h}, \mathbf{a}', \ell)], \quad (7)$$

where  $\mathbf{a}' = \mathbf{a}_{t+h:t+2h}$  denotes the next action chunk sampled from the current policy. Unlike standard  $n$ -step TD, the backup uses the exact action sequence that generated the intermediate rewards, eliminating the mismatch between the return estimator and the behavior policy. As a result, Q-chunking achieves

faster value propagation while preserving unbiased estimation [24].

In regions of the state-action space with insufficient observations, we find that traditional TD-based methods may extrapolate aggressively and produce overestimated action values. This effect is amplified in safety-critical manipulation tasks, where exploration is constrained and data diversity is inherently limited. To mitigate the overestimation arising from uncertainty, we employ a pessimistic ensemble of  $K$  action-value functions  $\{Q_{\phi_i}\}_{i=1}^K$ . Each critic is trained using the same chunked TD target in Eq. (7), by minimizing the objective:

$$\mathcal{L}_{\text{critic}} = \frac{1}{K} \sum_{i=1}^K \mathbb{E}_{\mathcal{D}} \left[ (Q_{\phi_i}(s_t, \mathbf{a}_{t:t+h}, \ell) - y_t^{(h)})^2 \right], \quad (8)$$

where  $y_t^{(h)}$  denotes the chunked TD target. At policy update time, we form a conservative estimate:

$$Q_{\text{pess}}(s_t, \mathbf{a}_{t:t+h}, \ell) = \min_i Q_{\phi_i}(s_t, \mathbf{a}_{t:t+h}, \ell), \quad (9)$$

which approximates a lower confidence bound on the true action value [9, 28]. This aggregation evaluates the current policy while providing more sensitive identification of uncertainty, improving robustness under real-world deployment.

### B. Advantage-Weighted Policy Improvement for VLA Policies

We now describe how the learned action-value function is used to update the VLA policy. Although the critic is learned off-policy, our value evaluation integrates naturally with the constrained policy update strategy used in RECAP [14], treating the critic as a relative preference signal. This preserves constraint updates and ensures stable policy improvement across online iterations. Given a transition, we evaluate the quality of the data action relative to the current policy  $\pi$  by defining the advantage:

$$A^\pi(s_t, \mathbf{a}_{t:t+h}, \ell) = Q_{\text{pess}}(s_t, \mathbf{a}_{t:t+h}, \ell) - \text{sg}(V^\pi(s_t, \ell)), \quad (10)$$

where  $V^\pi(s_t, \ell) = \mathbb{E}_{\mathbf{a}'_{t:t+h} \sim \pi_\theta(\cdot | s_t, \ell)} [Q_{\text{pess}}(s_t, \mathbf{a}'_{t:t+h}, \ell)]$  denotes the state-value function of the current policy. The stop-gradient operator  $\text{sg}$  prevents gradients from flowing through the last term, decoupling policy optimization from critic learning and improving training stability. By construction, this advantage provides a local, policy-dependent improvement signal that compares the action observed in the data against the behavior of the current policy at the same state and instruction. Policy improvement is performed via an advantage-weighted log-likelihood objective. To emphasize relative action quality while preserving stability, we transform the advantage into a non-negative weight using a clipped exponential,

$$w(s_t, \mathbf{a}_{t:t+h}, \ell) = \exp \left( \text{clip} \left( \frac{A^\pi(s_t, \mathbf{a}_{t:t+h}, \ell)}{\beta}, -\epsilon_{\text{clip}}, \epsilon_{\text{clip}} \right) \right), \quad (11)$$

where  $\beta$  controls the sharpness of the weighting and  $\epsilon_{\text{clip}}$  limits the maximum influence of any single transition, analogous to trust-region clipping in PPO-style updates [48]. The policy is

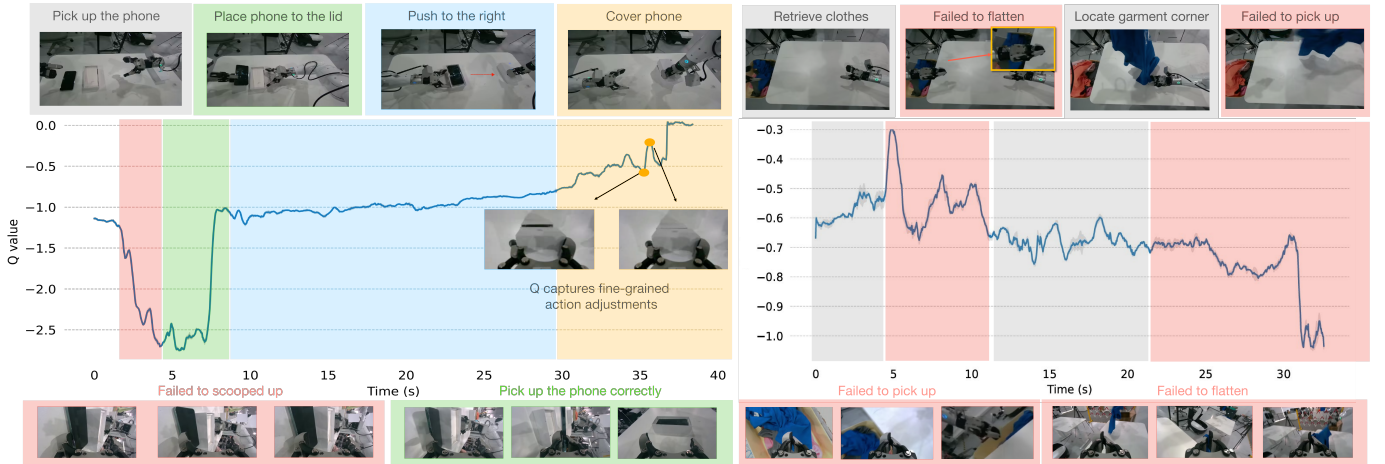


Fig. 3: **Visualization of Q-value.** Q-values predicted by the learned off-policy critic along a representative trajectory from the target policy (50Hz). The critic assigns sharply lower values to actions leading to failure and higher values to successful behaviors, demonstrating fine-grained action-level credit assignment in long-horizon manipulation tasks.

then updated by maximizing the weighted log-likelihood over the entire replay buffer,

$$\mathcal{L}_{\text{actor}} = \mathbb{E}_{\mathcal{D}} [w(s_t, \mathbf{a}_{t:t+h}, \ell) \log \pi_{\theta}(\mathbf{a}_{t:t+h} | s_t, \ell)]. \quad (12)$$

This update rule has several desirable properties. First, policy improvement is explicitly regularized. The policy is encouraged to increase the likelihood of actions observed in the data, which prevents uncontrolled extrapolation beyond the replay buffer. Second, because the advantage is defined relative to the current policy, the update focuses on correcting local deficiencies of the policy while remaining robust to global value estimation errors. These properties suggest that the update in Eq. (12) implements a conservative but principled policy improvement step:

**Theorem IV.1** (Constraint Policy Improvement). *For a given state  $s$ , let  $\pi_{\text{ref}}$  be the implicit behavior policy representing the data distribution in  $\mathcal{D}$ . The optimal solution to the advantage-weighted objective is the analytical solution to the following constrained optimization problem:*

$$\begin{aligned} \max_{\pi} \quad & \mathbb{E}_{\mathbf{a}_{t:t+h} \sim \pi(\cdot | s_t, \ell)} [Q(s_t, \mathbf{a}_{t:t+h}, \ell)] \\ \text{s.t.} \quad & D_{\text{KL}}(\pi(\cdot | s_t, \ell) \| \pi_{\text{ref}}(\cdot | s_t, \ell)) \leq \epsilon. \end{aligned} \quad (13)$$

The constraint  $\epsilon$  is implicitly controlled by the temperature parameter  $\beta$ .

Theorem IV.1 formalizes this interpretation by showing that the resulting policy update corresponds to the optimal solution of a constrained policy optimization problem, where improvement is explicitly restricted to the support of the data distribution.

### C. Implementation Details

We adopt the  $\pi_{0.5}$  flow-matching VLA model [4] as the actor. Given the visual observation, robot proprioception and language instruction, the actor predicts continuous action chunks

via the flow-matching action head. We fine-tune the actor end-to-end during RL. For critic, we adopt  $\pi_{0.5}$  pretrained SigLIP visual encoder [54] to extract image features, and fuse with other modalities using a Transformer backbone. To improve stability and reduce compute, we freeze the SigLIP encoder. We use an ensemble of  $K$  Q-functions implemented with  $K$  learnable Q readout tokens appended to the Transformer input sequence. Each readout token is mapped by an independent Q-head to predict a scalar Q value. We adopt a sparse terminal reward with a per-step penalty, following prior VLA RL practice [14]. For an episode terminating at step  $T$ , the reward is

$$r_t = \begin{cases} 0, & t = T \text{ and success} \\ -C_{\text{fail}}, & t = T \text{ and failure} \\ -1, & \text{otherwise,} \end{cases} \quad (14)$$

where we set  $C_{\text{fail}}$  to the average episode length according to the tasks.

Our actor parameterizes continuous action chunks via flow matching, so the continuous log-likelihood term in Eq. (12),  $\log \pi_{\theta}(\mathbf{a}_{t:t+h} | s_t, \ell)$ , is not tractable to evaluate exactly. Following prior flow/diffusion-style VLA training practice [14], we optimize a tractable surrogate by treating the negative flow-matching objective as a proxy for the continuous log-likelihood, i.e.,

$$\begin{aligned} \mathcal{L}_{\text{actor}} = \mathbb{E}_{\mathcal{D}} \left[ w(s_t, \mathbf{a}_{t:t+h}, \ell) \left\| \epsilon - \mathbf{a}_{t:t+h} - f_{\theta}(\tilde{\mathbf{a}}_{t:t+h}, s_t, \ell) \right\|_2^2 \right], \\ (s_t, \mathbf{a}_{t:t+h}, \ell) \sim \mathcal{D}, \quad \eta \sim \mathcal{U}[0, 1], \quad \epsilon \sim \mathcal{N}(\mathbf{0}, \mathbf{I}), \end{aligned} \quad (15)$$

where the noised action defined as  $\tilde{\mathbf{a}}_{t:t+h} = \eta \mathbf{a}_{t:t+h} + (1-\eta)\epsilon$ . Intuitively, maximizing the weighted policy log likelihood corresponds to minimizing weighted flow-matching loss for the action chunks under the same inputs. The state input to the actor and critic is  $s_t = [X_t^1, X_t^2, X_t^3, q_t]$ , where  $X_t^i$  denotes the image from the  $i$ -th camera and  $q_t$  denotes the

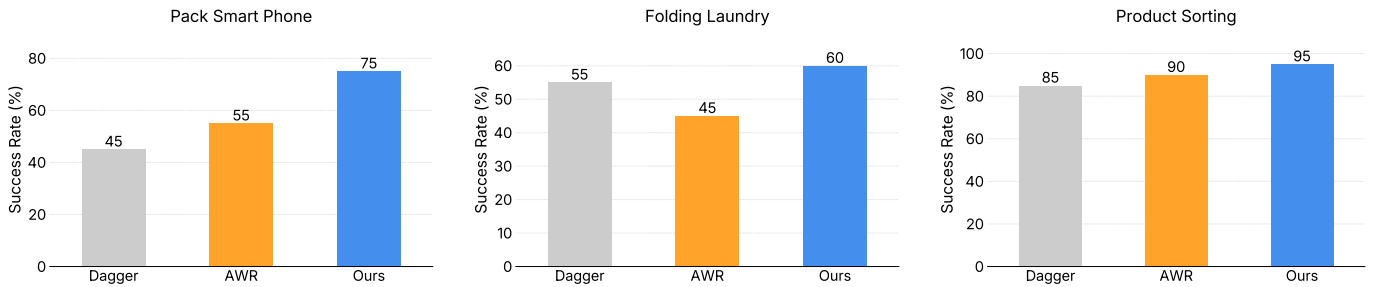


Fig. 4: **The average success rate of the three manipulation tasks.** We evaluate the baselines under real-world setting with several runs and calculate the average success rate.

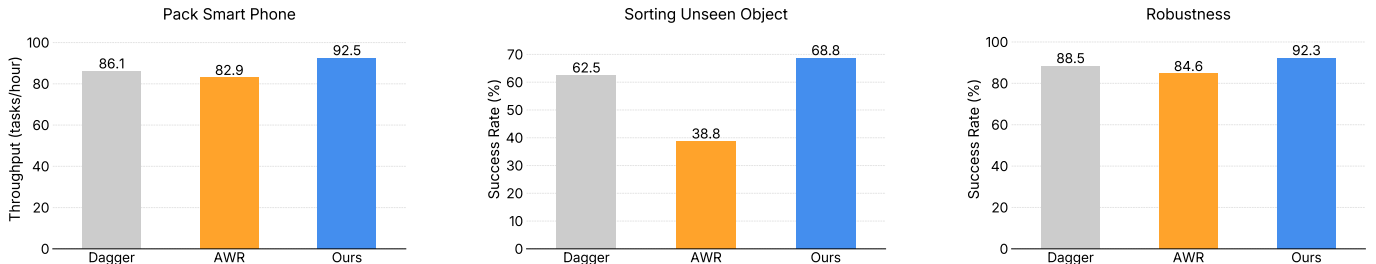


Fig. 5: **Evaluation of efficiency, zero-shot generalization, and robustness across tasks.** The left plot reports execution throughput on the phone-case task, where higher throughput indicates more efficient task completion. The middle plot evaluates generalization to unseen objects in a pick-and-place setting. The right plot measures robustness by injecting disturbances into the robot’s actions and assessing its ability to recover and successfully complete the task.

robot proprioceptive observation. More training details and parameter settings can be found on Appendix C.

## V. EXPERIMENTS

In this section, we evaluate ALOE on a set of real-world, robotic manipulation tasks designed to stress long-horizon reasoning, precise action selection, and robustness under human-in-the-loop data collection. Specifically, we consider three representative tasks: Pack Smart Phone, Folding Laundry, and Product Sorting. These tasks require a combination of fine-grained manipulation, multi-stage task composition (e.g., pick–place–push), and reasoning over visually ambiguous intermediate states. All experiments are conducted on a real robotic platform, illustrated in Fig. 2. More experimental implementation can be found on Appendix B.

### A. Description of Tasks

*a) Pack Smart Phone:* The Pack Smart Phone task requires the robot to align and attach a phone case onto a device body. Successful completion involves precise pose alignment, careful force control during insertion, and recovery from intermediate misalignment. The task is characterized by sparse rewards: the episode is marked successful only if the phone case is fully attached without collision-induced failure. Early termination is triggered when unsafe contact or irreversible misalignment is detected, often followed by human intervention. This task is particularly challenging for

trajectory-level value estimation, as failure is often caused by a single suboptimal action taken during a narrow time window.

*b) Folding Laundry:* Folding Laundry is a long-horizon manipulation task involving deformable object dynamics. The robot must grasp, lift, reposition, and fold a piece of cloth into a target configuration. This task emphasizes the need for precise grasp point selection, continuous visual feedback, and long-horizon planning to handle the highly variable shape and state of the cloth.

*c) Product Sorting:* The Product Sorting task requires the robot to identify, manipulate, and place multiple objects with diverse shapes and visual appearances into designated bins. The task involves object recognition, sequential decision-making, and collision-aware motion planning. Episodes may terminate early due to object drops or workspace violations. This setting evaluates the learning algorithm’s ability to generalize from fragmented experience and to assign credit to individual actions that influence downstream task success.

### B. Comparisons and Ablations

We compare ALOE against the following baselines:

- **BC ( $\pi_{0.5}$ ) [4]:** A pure imitation learning baseline trained on successful trajectories using the  $\pi_{0.5}$  architecture. This baseline reflects the performance achievable without reinforcement learning. The BC is used as warm up for all baselines.

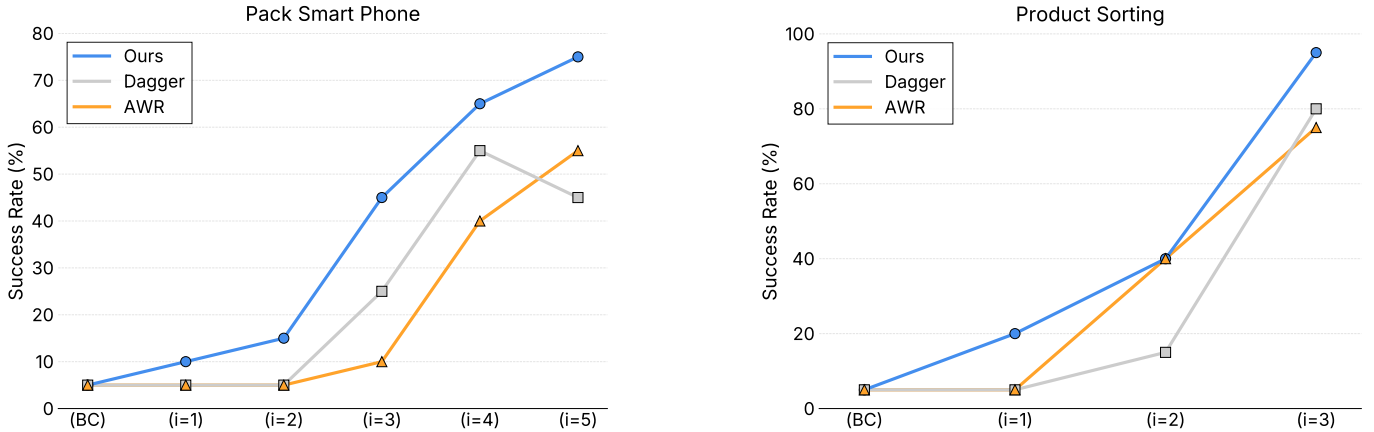


Fig. 6: **The performance of each RL iteration.** The success rates of ALOE on the Phone Case and Dual-Arm Object tasks increase consistently as RL training progresses, demonstrating stable policy improvement across online iterations.

- **Dagger [39]:** Based on the  $\pi_{0.5}$ , an iterative imitation learning method that aggregates online rollouts and human corrections. While effective at reducing covariate shift, DAgger does not explicitly leverage value estimation for long-term credit assignment.
- **AWR [36]:** An on-policy RL approach that uses Monte Carlo estimation to evaluate the reference policy in the replay buffer. AWR employs state-level value estimation and prioritizes robustness under real-world data collection but does not exploit action-level value information.

### C. Quantitative results

a) *What Does the Q-Function Actually Learn:* To better understand the role of the learned action-value function, We analyze the Q-value trend from a trajectory sampled from target policy in Fig. 3. For example, the color-coded regions on the left one correspond to behaviors critical for task success. The Q-value in the red region drops sharply when the robot fails to scoop up the phone, demonstrating the critic’s ability to identify failure modes. The Q-value in the green region increases sharply, indicating successful recovery behavior. The Q-value in the orange region increases gradually with fluctuations, assigning fine-grained credits to individual actions and providing richer supervision than trajectory-level value estimation.

b) *How much does ALOE improve the policy:* To evaluate the effectiveness of our off-policy algorithm, we compare task success rates across all methods, as summarized in Fig. 4. ALOE consistently outperforms all baselines on all three tasks, achieving higher success rates with fewer environment interactions compared to AWR, which demonstrates improved learning efficiency. For the Pack Smart Phone task, which requires high precision, we additionally measure throughput, which is the number of tasks completed per hour as shown in Fig. 5. Our method achieves higher throughput, indicating that the improved success rate translates to more efficient task execution in practice. For the Product Sorting task, we further

evaluate generalization performance on unseen objects. ALOE maintains robust performance on novel objects, demonstrating better generalization capability compared to baselines.

c) *How much does ALOE improve flow-based VLA over multiple iterations:* We evaluate how different learning methods improve a flow-based VLA policy across multiple training iterations, as shown in Fig. 6. Consistent with prior work, AWR yields noticeable gains over pure imitation learning in early iterations by stabilizing policy updates under real-world data collection. However, its improvements tend to steady and saturate as training progresses, particularly in tasks with delayed or action-specific failure modes such as Folding Laundry. In contrast, ALOE continues to improve the same flow-based VLA backbone over successive iterations, achieving higher final success rates and better sample efficiency. This result indicates that action-level off-policy value estimation provides additional learning signal beyond trajectory-level preference modeling when refining flow-based VLA policies.

## VI. CONCLUSION

In this paper, we analyze how value functions can be more effectively leveraged in real-world VLA RL. We propose ALOE, an action-level off-policy value estimation method that enables policy improvement while preserving robustness. Empirically, we demonstrate that off-policy, Bellman-based action-value estimation can be made reliable under human-in-the-loop data collection, and that ALOE consistently improves learning efficiency and task throughput over prior conservative VLA training methods across three real-world manipulation tasks. In future work, we plan to explore combining powerful off-policy value estimation with automated task and environment reset pipelines to enable fully autonomous real-world VLA training.

## REFERENCES

- [1] AgiBot-World-Contributors, Qingwen Bu, Jisong Cai, Li Chen, Xiuqi Cui, Yan Ding, Siyuan Feng, Shenyan

- Gao, Xindong He, Xuan Hu, Xu Huang, Shu Jiang, Yuxin Jiang, Cheng Jing, Hongyang Li, Jialu Li, Chiming Liu, Yi Liu, Yuxiang Lu, Jianlan Luo, Ping Luo, Yao Mu, Yuehan Niu, Yixuan Pan, Jiangmiao Pang, Yu Qiao, Guanghui Ren, Cheng Ruan, Jiaqi Shan, Yongjian Shen, Chengshi Shi, Mingkang Shi, Modi Shi, Chonghao Sima, Jianheng Song, Huijie Wang, Wenhao Wang, Dafeng Wei, Chengen Xie, Guo Xu, Junchi Yan, Cunbiao Yang, Lei Yang, Shukai Yang, Maoqing Yao, Jia Zeng, Chi Zhang, Qinglin Zhang, Bin Zhao, Chengyue Zhao, Jiaqi Zhao, and Jianchao Zhu. Agibot world colosseum: A large-scale manipulation platform for scalable and intelligent embodied systems, 2025. URL <https://arxiv.org/abs/2503.06669>.
- [2] Marc G Bellemare, Will Dabney, and Rémi Munos. A distributional perspective on reinforcement learning. In *International conference on machine learning*, pages 449–458. PMLR, 2017.
- [3] Dimitri Bertsekas. *Dynamic programming and optimal control: Volume I*, volume 4. Athena scientific, 2012.
- [4] Kevin Black, Noah Brown, James Darphinian, Karan Dhabalia, Danny Driess, Adnan Esmail, Michael Robert Equi, Chelsea Finn, Niccolo Fusai, Manuel Y. Galiker, Dibya Ghosh, Lachy Groom, Karol Hausman, Brian Ichter, Szymon Jakubczak, Tim Jones, Liyiming Ke, Devin LeBlanc, Sergey Levine, Adrian Li-Bell, Mohith Mothukuri, Suraj Nair, Karl Pertsch, Allen Z. Ren, Lucy Xiaoyang Shi, Laura Smith, Jost Tobias Springenberg, Kyle Stachowicz, James Tanner, Quan Vuong, Homer Walke, Anna Walling, Haohuan Wang, Lili Yu, and Ury Zhilinsky.  $\pi_{0.5}$ : a vision-language-action model with open-world generalization. In *9th Annual Conference on Robot Learning*, 2025. URL <https://openreview.net/forum?id=vlhsoswksBO>.
- [5] Kevin Black, Noah Brown, Danny Driess, Adnan Esmail, Michael Robert Equi, Chelsea Finn, Niccolo Fusai, Lachy Groom, Karol Hausman, Brian Ichter, Szymon Jakubczak, Tim Jones, Liyiming Ke, Sergey Levine, Adrian Li-Bell, Mohith Mothukuri, Suraj Nair, Karl Pertsch, Lucy Xiaoyang Shi, Laura Smith, James Tanner, Quan Vuong, Anna Walling, Haohuan Wang, and Ury Zhilinsky.  $\pi_0$ : A Vision-Language-Action Flow Model for General Robot Control. In *Proceedings of Robotics: Science and Systems*, Los Angeles, CA, USA, June 2025. doi: 10.15607/RSS.2025.XXI.010.
- [6] Kang Chen, Zhihao Liu, Tonghe Zhang, Zhen Guo, Si Xu, Hao Lin, Hongzhi Zang, Quanlu Zhang, Zhaofei Yu, Guoliang Fan, Tiejun Huang, Yu Wang, and Chao Yu.  $\pi_{r1}$ : Online rl fine-tuning for flow-based vision-language-action models. *arXiv preprint*, arXiv:2510.25889, 2025.
- [7] Yuhui Chen, Shuai Tian, Shugao Liu, Yingting Zhou, Haoran Li, and Dongbin Zhao. Conrft: A reinforced fine-tuning method for vla models via consistency policy. *arXiv preprint arXiv:2502.05450*, 2025.
- [8] Kevin Frans, Seohong Park, Pieter Abbeel, and Sergey Levine. Diffusion guidance is a controllable policy improvement operator. *arXiv preprint*, arXiv:2505.23458, 2025.
- [9] Kamyar Ghasemipour, Shixiang Shane Gu, and Ofir Nachum. Why so pessimistic? estimating uncertainties for offline rl through ensembles, and why their independence matters. *Advances in Neural Information Processing Systems*, 35:18267–18281, 2022.
- [10] Seyed Kamyar Ghasemipour, Ayzaan Wahid, Jonathan Tompson, Pannag Sanketi, and Igor Mordatch. Self-improving embodied foundation models. *arXiv preprint*, arXiv:2509.15155, 2025.
- [11] Tuomas Haarnoja, Aurick Zhou, Pieter Abbeel, and Sergey Levine. Soft actor-critic: Off-policy maximum entropy deep reinforcement learning with a stochastic actor. In *International Conference on Machine Learning*, pages 1861–1870. Pmlr, 2018.
- [12] David Hoeller, Nikita Rudin, Dhionis Sako, and Marco Hutter. Anymal parkour: Learning agile navigation for quadrupedal robots. *Science Robotics*, 9(88):eadi7566, 2024.
- [13] Dongchi Huang, Zhirui Fang, Tianle Zhang, Yihang Li, Lin Zhao, and Chunhe Xia. Co-rft: Efficient fine-tuning of vision-language-action models through chunked offline reinforcement learning. *arXiv preprint*, arXiv:2508.02219, 2025.
- [14] Physical Intelligence, Ali Amin, Raichelle Aniceto, Ashwin Balakrishna, Kevin Black, Ken Conley, Grace Connors, James Darphinian, Karan Dhabalia, Jared DiCarlo, et al.  $\pi_{0.6}^*$ : a vla that learns from experience. *arXiv preprint arXiv:2511.14759*, 2025.
- [15] Steeven Janny, Hervé Poirier, Leonid Antsfeld, Guillaume Bono, Gianluca Monaci, Boris Chidlovskii, Francesco Giuliani, Alessio Del Bue, and Christian Wolf. Reasoning in visual navigation of end-to-end trained agents: a dynamical systems approach. In *Proceedings of the Computer Vision and Pattern Recognition Conference*, pages 12111–12121, 2025.
- [16] Dmitry Kalashnikov, Alex Irpan, Peter Pastor, Julian Ibarz, Alexander Herzog, Eric Jang, Deirdre Quillen, Ethan Holly, Mrinal Kalakrishnan, Vincent Vanhoucke, et al. QT-Opt: Scalable deep reinforcement learning for vision-based robotic manipulation. *arXiv preprint arXiv:1806.10293*, 2018.
- [17] Michael Kelly, Chelsea Sidrane, Katherine Driggs-Campbell, and Mykel J. Kochenderfer. Hg-dagger: Interactive imitation learning with human experts, 2019. URL <https://arxiv.org/abs/1810.02890>.
- [18] Jakub Grudzien Kuba, Pieter Abbeel, and Sergey Levine. Advantage-conditioned diffusion: Offline rl via generalization, 2024. URL <https://openreview.net/forum?id=QDrG0ALeVs>.
- [19] Aviral Kumar, Justin Fu, Matthew Soh, George Tucker, and Sergey Levine. Stabilizing off-policy q-learning via bootstrapping error reduction. In *NeurIPS*, pages 11784–11794, 2019.

- [20] Michael Laskey, Jonathan Lee, Roy Fox, Anca Dragan, and Ken Goldberg. Shiv: Reducing supervisor burden in dagger using support vectors for efficient learning from demonstrations in high dimensional state spaces. In *Proceedings of the 2016 IEEE International Conference on Robotics and Automation (ICRA)*, pages 462–469, 2016. doi: 10.1109/ICRA.2016.7487175.
- [21] Sergey Levine, Chelsea Finn, Trevor Darrell, and Pieter Abbeel. End-to-end training of deep visuomotor policies. *The Journal of Machine Learning Research*, 17(1):1334–1373, 2016.
- [22] Haozhan Li, Yuxin Zuo, Jiale Yu, Yuhao Zhang, Zhaohui Yang, Kaiyan Zhang, Xuekai Zhu, Yuchen Zhang, Tianxing Chen, Ganqu Cui, Dehui Wang, Dingxiang Luo, Yuchen Fan, Youbang Sun, Jia Zeng, Jiangmiao Pang, Shanghang Zhang, Yu Wang, Yao Mu, Bowen Zhou, and Ning Ding. Simplevla-rl: Scaling vla training via reinforcement learning. *arXiv preprint*, arXiv:2509.09674, 2025.
- [23] Haozhan Li, Yuxin Zuo, Jiale Yu, Yuhao Zhang, Zhaohui Yang, Kaiyan Zhang, Xuekai Zhu, Yuchen Zhang, Tianxing Chen, Ganqu Cui, et al. Simplevla-rl: Scaling vla training via reinforcement learning. *arXiv preprint arXiv:2509.09674*, 2025.
- [24] Qiyang Li, Zhiyuan Zhou, and Sergey Levine. Reinforcement learning with action chunking. *arXiv preprint arXiv:2507.07969*, 2025.
- [25] Xiaoqi Li, Mingxu Zhang, Yiran Geng, Haoran Geng, Yuxing Long, Yan Shen, Renrui Zhang, Jiaming Liu, and Hao Dong. Manipllm: Embodied multimodal large language model for object-centric robotic manipulation. In *Proceedings of the IEEE/CVF Conference on Computer Vision and Pattern Recognition*, pages 18061–18070, 2024.
- [26] Ji Lin, Hongxu Yin, Wei Ping, Pavlo Molchanov, Mohammad Shoeybi, and Song Han. Vila: On pre-training for visual language models. In *Proceedings of the IEEE/CVF conference on computer vision and pattern recognition*, pages 26689–26699, 2024.
- [27] Jijia Liu, Feng Gao, Bingwen Wei, Xinlei Chen, Qingmin Liao, Yi Wu, Chao Yu, and Yu Wang. What can rl bring to vla generalization? an empirical study. *arXiv preprint*, arXiv:2505.19789, 2025.
- [28] Owen Lockwood and Mei Si. A review of uncertainty for deep reinforcement learning. In *Proceedings of the AAAI Conference on Artificial Intelligence and Interactive Digital Entertainment*, volume 18, pages 155–162, 2022.
- [29] Guanxing Lu, Wenkai Guo, Chubin Zhang, Yuheng Zhou, Haonan Jiang, Zifeng Gao, Yansong Tang, and Ziwei Wang. Vla-rl: Towards masterful and general robotic manipulation with scalable reinforcement learning. *arXiv preprint*, arXiv:2505.18719, 2025.
- [30] Jianlan Luo, Zheyuan Hu, Charles Xu, You Liang Tan, Jacob Berg, Archit Sharma, Stefan Schaal, Chelsea Finn, Abhishek Gupta, and Sergey Levine. Serl: A software suite for sample-efficient robotic reinforcement learning, 2024.
- [31] Yecheng Jason Ma, William Liang, Vaidehi Som, Vikash Kumar, Amy Zhang, Osbert Bastani, and Dinesh Jayaraman. Liv: Language-image representations and rewards for robotic control. In *Proceedings of the 40th International Conference on Machine Learning (ICML)*, 2023.
- [32] Yecheng Jason Ma, Joey Hejna, Ayzaan Wahid, Chuyuan Fu, Dhruv Shah, Jacky Liang, Zhuo Xu, Sean Kirmani, Peng Xu, Danny Driess, Ted Xiao, Jonathan Tompson, Osbert Bastani, Dinesh Jayaraman, Wenhao Yu, Tingnan Zhang, Dorsa Sadigh, and Fei Xia. Vision language models are in-context value learners, 2024.
- [33] Yecheng Jason Ma, Joey Hejna, Chuyuan Fu, Dhruv Shah, Jacky Liang, Zhuo Xu, Sean Kirmani, Peng Xu, Danny Driess, Ted Xiao, Osbert Bastani, Dinesh Jayaraman, Wenhao Yu, Tingnan Zhang, Dorsa Sadigh, and Fei Xia. Vision language models are in-context value learners. In *Proceedings of the 13th International Conference on Learning Representations (ICLR)*, 2025.
- [34] Kunal Menda, Katherine Driggs-Campbell, and Mykel J Kochenderfer. Ensembledagger: A bayesian approach to safe imitation learning. In *IROS*, 2019.
- [35] Russell Mendonca, Shikhar Bahl, and Deepak Pathak. Alan: Autonomously exploring robotic agents in the real world. In *Proceedings of the 2023 IEEE International Conference on Robotics and Automation (ICRA)*, pages 3044–3050, 2023. doi: 10.1109/ICRA48891.2023.10013321.
- [36] Xue Bin Peng, Aviral Kumar, Grace Zhang, and Sergey Levine. Advantage-weighted regression: Simple and scalable off-policy reinforcement learning. *arXiv preprint arXiv:1910.00177*, 2019.
- [37] Allen Z. Ren, Justin Lidard, Lars L. Ankile, Anthony Simeonov, Pulkit Agrawal, Anirudha Majumdar, Benjamin Burchfiel, Hongkai Dai, and Max Simchowitz. Diffusion policy policy optimization. In *arXiv preprint arXiv:2409.00588*, 2024.
- [38] Allen Z. Ren, Justin Lidard, Lars Lien Ankile, Anthony Simeonov, Pulkit Agrawal, Anirudha Majumdar, Benjamin Burchfiel, Hongkai Dai, and Max Simchowitz. Diffusion Policy Policy Optimization. In *Proceedings of the 2025 International Conference on Learning Representations (ICLR)*, 2025.
- [39] Stéphane Ross, Geoffrey Gordon, and Drew Bagnell. A reduction of imitation learning and structured prediction to no-regret online learning. In *AISTATS*, pages 627–635, 2011.
- [40] Zhihong Shao, Peiyi Wang, Qihao Zhu, Runxin Xu, Junxiao Song, Xiao Bi, Haowei Zhang, Mingchuan Zhang, YK Li, Yang Wu, et al. Deepseekmath: Pushing the limits of mathematical reasoning in open language models. *arXiv preprint arXiv:2402.03300*, 2024.
- [41] Archit Sharma, M. Ahmed Ahmed Rehaan Ahmad, and Chelsea Finn. Self-improving robots: End-to-end autonomous visuomotor reinforcement learning. In

- Proceedings of the 7th Conference on Robot Learning (CoRL)*, volume 229, pages 3292–3308. PMLR, 2023.
- [42] Richard S Sutton. Learning to predict by the methods of temporal differences. *Machine learning*, 3(1):9–44, 1988.
- [43] Richard S Sutton, Andrew G Barto, et al. *Reinforcement learning: An introduction*, volume 1. MIT press Cambridge, 1998.
- [44] Andrew Szot, Bogdan Mazouze, Omar Attia, Aleksei Timofeev, Harsh Agrawal, Devon Hjelm, Zhe Gan, Zsolt Kira, and Alexander Toshev. From multimodal llms to generalist embodied agents: Methods and lessons. In *Proceedings of the Computer Vision and Pattern Recognition Conference*, pages 10644–10655, 2025.
- [45] Shuhan Tan, Kairan Dou, Yue Zhao, and Philipp Krähenbühl. Interactive post-training for vision-language-action models. *arXiv preprint*, arXiv:2505.17016, 2025.
- [46] Generalist AI Team. Gen-0: Embodied foundation models that scale with physical interaction. *Generalist AI Blog*, 2025. <https://generalistai.com/blog/nov-04-2025-GEN-0>.
- [47] Hado Van Hasselt, Yotam Doron, Florian Strub, Matteo Hessel, Nicolas Sonnerat, and Joseph Modayil. Deep reinforcement learning and the deadly triad. *arXiv preprint arXiv:1812.02648*, 2018.
- [48] Yuhui Wang, Hao He, and Xiaoyang Tan. Truly proximal policy optimization. In Ryan P. Adams and Vibhav Gogate, editors, *Proceedings of The 35th Uncertainty in Artificial Intelligence Conference*, volume 115 of *Proceedings of Machine Learning Research*, pages 113–122. PMLR, 22–25 Jul 2020. URL <https://proceedings.mlr.press/v115/wang20b.html>.
- [49] Ronald J Williams. Simple statistical gradient-following algorithms for connectionist reinforcement learning. *Machine learning*, 8(3-4):229–256, 1992.
- [50] Philipp Wu, Yide Shentu, Qiayuan Liao, Ding Jin, Menglong Guo, Koushil Sreenath, Xingyu Lin, and Pieter Abbeel. Robocopilot: Human-in-the-loop interactive imitation learning for robot manipulation, 2025. URL <https://arxiv.org/abs/2503.07771>.
- [51] Charles Xu, Qiyang Li, Jianlan Luo, and Sergey Levine. RLDG: robotic generalist policy distillation via reinforcement learning. *CoRR*, abs/2412.09858, 2024. doi: 10.48550/ARXIV.2412.09858.
- [52] Jianwei Yang, Reuben Tan, Qianhui Wu, Ruijie Zheng, Baolin Peng, Yongyuan Liang, Yu Gu, Mu Cai, Seonghyeon Ye, Joel Jang, et al. Magma: A foundation model for multimodal ai agents. In *Proceedings of the Computer Vision and Pattern Recognition Conference*, pages 14203–14214, 2025.
- [53] Shaopeng Zhai, Qi Zhang, Tianyi Zhang, Fuxian Huang, Haoran Zhang, Ming Zhou, Shengzhe Zhang, Litao Liu, Sixu Lin, and Jiangmiao Pang. A vision-language-action-critic model for robotic real-world reinforcement learning. *arXiv preprint*, arXiv:2509.15937, 2025.
- [54] Xiaohua Zhai, Basil Mustafa, Alexander Kolesnikov, and Lucas Beyer. Sigmoid loss for language image pre-training. In *International Conference on Computer Vision (ICCV)*, 2023.
- [55] Tonghe Zhang, Chao Yu, Sichang Su, and Yu Wang. Reinfo: Fine-tuning flow matching policy with online reinforcement learning, 2026. URL <https://arxiv.org/abs/2505.22094>.
- [56] Yixian Zhang, Shu’ang Yu, Tonghe Zhang, Mo Guang, Haojia Hui, Kaiwen Long, Yu Wang, Chao Yu, and Wenbo Ding. Sac flow: Sample-efficient reinforcement learning of flow-based policies via velocity-reparameterized sequential modeling, 2026. URL <https://arxiv.org/abs/2509.25756>.
- [57] Qingqing Zhao, Yao Lu, Moo Jin Kim, Zipeng Fu, Zhuoyang Zhang, Yecheng Wu, Zhaoshuo Li, Qianli Ma, Song Han, Chelsea Finn, et al. Cot-vla: Visual chain-of-thought reasoning for vision-language-action models. In *Proceedings of the Computer Vision and Pattern Recognition Conference*, pages 1702–1713, 2025.

## APPENDIX

This appendix provides detailed information for reproducibility, including platform setup, task specifications, human-in-the-loop data collection, and training configurations.

### A. Robotic Platform

We describe the robotic platform and perception setup used for all tasks. Our experimental platform is built on the Agibot robotic system, which consists of dual 7-DoF manipulator arms mounted on a mobile base with an adjustable waist mechanism. The platform supports modular end-effectors, enabling flexible configuration with either standard grippers or 6-DoF dexterous hands depending on the task requirements. The perception system includes multiple camera modalities: an RGB camera providing front-view coverage, along with RGB cameras mounted on each end-effector for close-up manipulation views. This multi-camera setup enables comprehensive visual observation from both global and local perspectives, which is essential for fine-grained manipulation tasks. For human-in-the-loop data collection, we employ VR-based teleoperation control. The operator uses a VR headset and controllers to command the robot. The VR controller hand gestures are mapped to end-effector translations and rotations, which are then converted to joint angle commands through inverse kinematics. The controller thumbsticks and buttons enable base and body movement control, while trigger buttons actuate the end-effectors. This teleoperation interface allows operators to provide real-time demonstrations, reset and interventions during policy rollouts, enabling the collection of high-quality demonstration data and safety interventions when needed.

### B. Post-training Process under Human-in-the-Loop Data Collection

We describe our post-training process under a human-in-the-loop setting. For each task, we first collect several human demonstrations and use them to warm-start  $\pi_{0.5}$  via imitation learning. At each RL iteration, we roll out  $\pi_{0.5}$  while a human monitors execution. The human intervenes via teleoperation when unsafe behaviors are imminent, such as dropping or damaging the phone, which triggers early termination. If the policy fails or times out, the human resets the environment to the failure state and demonstrates corrective actions to complete the task. All trajectories, including both autonomous executions and human interventions, are stored in the replay buffer. The resulting dataset contains both successful and failed fragments, reflecting the heterogeneous nature of human-in-the-loop data collection. Data collection continues until a fixed number of successful trajectories is reached (e.g., 50 for the phone task). We then apply ALOE (Algorithm 1) to update the critic and actor before proceeding to the next RL iteration. Human intervention is frequent in early iterations but decreases as the policy improves.

### C. Training Details and Hyperparameters

We summarize the actor architecture, critic design, optimization settings, and baseline implementations.

1) *ALOE Actor*: We use the  $\pi_{0.5}$  flow-matching VLA model [4] as the policy backbone, containing approximately 3B parameters. Policies are fine-tuned end-to-end. At deployment, inference runs on a single RTX 4090 GPU. The control frequency is 30 Hz, and manipulators operate under asynchronous control to reduce latency.

2) *ALOE Critic*: We employ a Transformer-based multi-modal critic to estimate chunked action-values. Visual observations are encoded using a pretrained SigLIP encoder, which remains frozen for stability. Proprioception and action chunks are projected into a shared embedding space of dimension  $D = 256$ . An ensemble of  $K$  Q-tokens is prepended to the input sequence as readout tokens, each mapped to a scalar Q-value via an independent MLP head. The input sequence is

$$\mathbf{X} = [\mathbf{q}_1, \dots, \mathbf{q}_K, \mathbf{s}, \mathbf{a}_1, \dots, \mathbf{a}_h, \mathbf{x}_1, \dots, \mathbf{x}_V],$$

where  $h = 50$  and  $V = 3$ , giving sequence length  $L = 56$ . The Transformer uses 6 layers and 8 attention heads. The critic is trained with Q-chunking TD targets (Eq. 7) and pessimistic aggregation. Target networks are updated via Polyak averaging with coefficient 0.005. Optimization uses AdamW with  $\beta_1 = 0.9$ ,  $\beta_2 = 0.95$ , cosine learning-rate schedule (peak  $3 \times 10^{-5}$ , 100 warmup steps), gradient clipping at 1.0, discount factor  $\gamma = 0.99$ , and batch size 256.

3) *Baselines*: All baselines use the same  $\pi_{0.5}$  backbone for fair comparison. For sorting and phone packing, training starts from an open-source checkpoint. For laundry folding, we warm-start with additional task data due to task difficulty.

**Behavior Cloning (BC)**. We follow [4] and minimize the flow-matching objective:

$$\mathcal{L}_{\text{BC}} = \mathbb{E}_{\mathcal{D}} \|\epsilon - \mathbf{a}_{t:t+h} - f_{\theta}(\tilde{\mathbf{a}}_{t:t+h}, s_t, \ell)\|_2^2, \quad (16)$$

**Dagger**. We implement human-in-the-loop DAgger [17, 34, 39]. Each iteration aggregates new demonstrations and trains with the same objective as BC.

**AWR**. We follow [36] and implement a distributional value critic [2] with  $N = 256$  bins. The value distribution is:

$$p_{\theta}(V|s) = (p_0, \dots, p_N),$$

and

$$V(s) = \sum_i z_i \frac{e^{p_i}}{\sum_j e^{p_j}}.$$

Targets are Monte Carlo returns discretized between  $V_{\min}$  and  $V_{\max}$ . The critic shares the same architecture as the ALOE critic but uses a single head ( $K = 1$ ).

4) *Optimization Settings*: Replay buffers accumulate data across iterations:

$$D_i^{\text{replay}} = D_{i-1} \cup \mathcal{D}_i^{\text{replay}}.$$

Both ALOE and AWR critics/actors are continually fine-tuned from the previous iteration, following standard continual policy refinement practice in human-in-the-loop learning [50]. Policies are evaluated using their respective critics.

### D. Tasks and Environments

We evaluate on three real-world manipulation tasks.

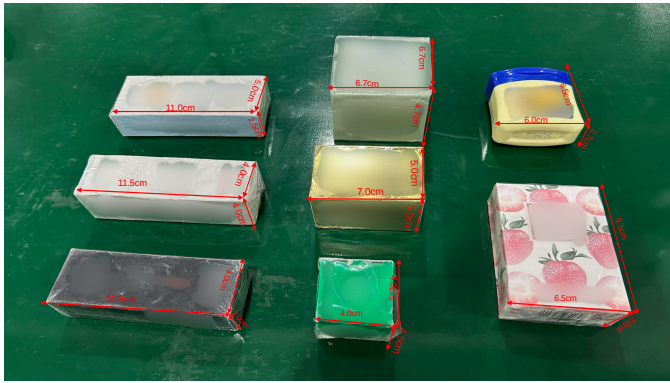


Fig. 7: Objects used for zero-shot generalization evaluation on the Product Sorting task.

1) *Pack Smart Phone*: Pack Smart Phone is a bimanual fine-manipulation task: pick the phone from the table, place it fully inside a rigid container (17.5cm  $\times$  8.6cm), position the container, and close the lid. The phone case (17.8cm  $\times$  8.8cm) has minimal clearance, making insertion and lid closure precision-critical. Success requires continuous pose alignment and recovery from positional variability during placement. We use joint angles and gripper pose as the action output.

TABLE I: Task parameters for Pack Smart Phone task.

Parameter	Value
Action space	14-dimensional
Observation space	RGB from left/right wrist camera, RGB from head camera, 32 proprio
Prompt	Place the phone in the container, then cover it with the lid
Initial offline demonstrations	50
Max episode length	2000
Action chunk length	50
Execution chunk length	25
Reset method	Human reset
Randomization range	3 cm in x and y

The reward function is defined as follows:

- **Success**: If the phone is completely placed in the container and the lid is successfully closed, the reward is 0.
- **Intermediate steps**: The intermediate process receives a reward of -1.
- **Failure cases**: The reward is  $-C_{\text{fail}}$  if the phone accidentally drops, fails to accurately insert into the container, causes damage during insertion, or if the time step exceeds the max episode length.

2) *Folding Laundry*: Folding Laundry is a bimanual long-horizon task with deformable objects. The robot retrieves a garment from a rigid basket (35.0cm  $\times$  24.0cm), flattens it via coordinated bimanual grasping and spreading, then executes sequential folds to a target configuration. Garments vary in color (six types) and size, demanding robust visual perception and generalization of folding strategies. The high-dimensional

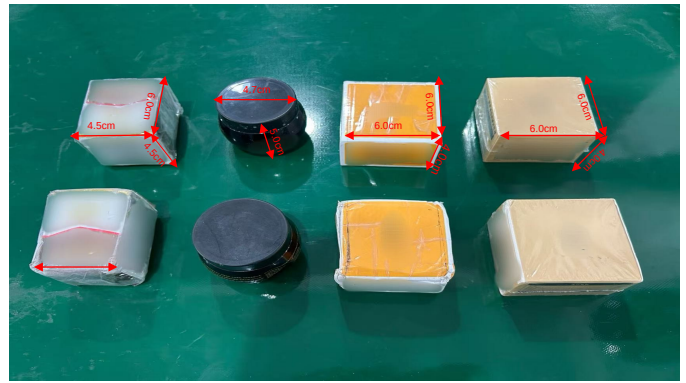


Fig. 8: Objects used for training on the Product Sorting task.

configuration space and long episode duration necessitate recovery from entanglement and irregular states.

TABLE II: Task parameters for Folding Laundry task.

Parameter	Value
Action space	14-dimensional
Observation space	RGB from left/right wrist camera, RGB from head camera, 32 proprio
Prompt	Fold the t-shirt
Initial offline demonstrations	150
Max episode length	10000
Action chunk length	50
Execution chunk length	5
Reset method	Human reset
Randomization range	Randomly place clothes in the box

The reward function is defined as follows:

- **Success**: If the clothes are neatly folded, the reward is 0.
- **Intermediate steps**: The intermediate process receives a reward of -1.
- **Failure cases**: The reward is  $-C_{\text{fail}}$  if the gripper performs an empty grasp or grasps multiple layers of clothes, if the robot repeatedly shakes the clothes, if the robot begins folding without flattening the garment first, if the robot collides with the table, if the robot re-flattens the garment during the folding process, or if the time step exceeds the max episode length.

3) *Product Sorting*: Product Sorting is a bimanual pick-place task. The robot empties two material bins (left and right) by picking objects and placing them onto a front conveyor belt. Each arm is constrained to its own bin (left gripper from left bin, right from right); the task is complete when both bins are empty.

The reward function is defined as follows:

- **Success**: If both material bins are successfully emptied, the reward is 0.
- **Intermediate steps**: The intermediate process receives a reward of -1.
- **Failure cases**: The reward is  $-C_{\text{fail}}$  if any of the following situations occur: gripper positioning failure, empty gripper grasp, the gripper squeezing other objects during the grasping process, the robotic arm colliding with the

TABLE III: Task parameters for Product Sorting task.

Parameter	Value
Action space	14-dimensional
Observation space	RGB from left/right wrist camera, RGB from head camera, 32 proprio
Prompt	Retrieve the objects from the front bin and place them onto the conveyor belt.
Initial offline demonstrations	50
Max episode length	10000
Action chunk length	50
Execution chunk length	5
Reset method	Human reset
Randomization range	Randomly place objects in the bins

material bin during movement, the gripper releasing the material in advance while the material is still in the air, collision occurring during the gripper placement process, or the time step exceeding the maximum episode length.

### E. Evaluation Protocol

We define success rate, throughput, unseen object evaluation, and robustness protocol.

**Success rate.** Success rate is the fraction of successful episodes over the total number of evaluation episodes across multiple evaluation rounds. An episode is considered successful when the task is completed according to the reward-defined success criteria; it is considered completed (for throughput) when it terminates due to success, failure, or timeout.

**Throughput.** Throughput is defined as completed episodes per hour and captures both execution speed and reliability under a fixed time budget. Throughput is measured as policy-side throughput only: time for environment reset and scene setup between trials by the human operator is excluded. This exclusion is applied consistently across all compared methods, so relative throughput comparisons remain valid (Fig. 5, left).

**Unseen object zero-shot generalization.** To evaluate generalization to novel objects, we replace the objects in the Product Sorting task with objects that were never seen during training (different shapes and colors). See Fig. 8 and Fig. 7 for examples of training vs. unseen objects. The policy is evaluated without fine-tuning; this setting assesses the VLA’s ability to generalize to unseen object appearances and geometries (Fig. 5, middle).

**Robustness evaluation.** During evaluation, we inject random perturbations to the garment being manipulated (e.g., in Folding Laundry) while the policy is executing. We then measure whether the VLA can re-adjust its actions and still complete the task successfully. This protocol evaluates recovery from unexpected disturbances (Fig. 5, right).

### F. Additional Results

Table IV reports the performance of behavior cloning (BC) on the three tasks. All baselines start from the bc checkpoint before iterative RL. Fig. 9 provides an additional visualization of the learned  $Q(s, a)$  along a trajectory.

TABLE IV: BC performance on three tasks.

	Pack Phone	Folding Laundry	Object Sorting
BC	5.0	15.0	5.0

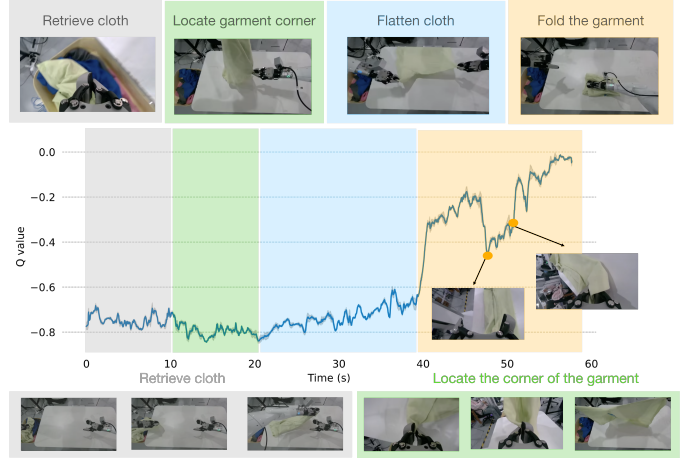


Fig. 9: Additional  $Q(s, a)$  visualization along a representative trajectory.

### G. Proof of Policy Improvement

The following proof formalizes the connection between the advantage-weighted actor objective and the KL-constrained policy improvement problem.

*Proof:* Fix a state  $s$  (and omit  $\ell$  for brevity). Consider the KL-constrained policy improvement problem:

$$\begin{aligned}
 & \max_{\pi} \int \pi(a) Q(a) da \\
 & \text{s.t.} \int \pi(a) \log \frac{\pi(a)}{\pi_{\text{ref}}(a)} da \leq \epsilon, \\
 & \int \pi(a) da = 1.
 \end{aligned} \tag{17}$$

Form the Lagrangian

$$\begin{aligned}
 \mathcal{L}(\pi, \beta, \alpha) = & \int \pi(a) Q(a) da \\
 & - \beta \left( \int \pi(a) \log \frac{\pi(a)}{\pi_{\text{ref}}(a)} da - \epsilon \right) \\
 & + \alpha \left( \int \pi(a) da - 1 \right).
 \end{aligned} \tag{18}$$

Taking the functional derivative and setting it to zero:

$$\frac{\delta \mathcal{L}}{\delta \pi(a)} = Q(a) - \beta \left( \log \frac{\pi(a)}{\pi_{\text{ref}}(a)} + 1 \right) + \alpha = 0, \tag{19}$$

which yields

$$\pi^*(a) \propto \pi_{\text{ref}}(a) \exp\left(\frac{Q(a)}{\beta}\right). \tag{20}$$

Now consider the advantage-weighted objective in Eq. (12):

$$\mathbb{E}_{a \sim \pi_{\text{ref}}} \left[ \exp(A^\pi(a)/\beta) \log \pi_\theta(a) \right].$$

Since

$$A^\pi(a) = Q(a) - V^\pi(s),$$

and  $V^\pi(s)$  is constant w.r.t.  $a$ , the weighting is proportional to  $\exp(Q(a)/\beta)$ . Therefore, the maximum-likelihood solution satisfies

$$\pi_\theta(a) \propto \pi_{\text{ref}}(a) \exp\left(\frac{Q(a)}{\beta}\right), \quad (21)$$

which matches the solution to the KL-constrained problem. Hence Eq. (12) implements the optimal constraint policy improvement. ■